IJBPAS, August, 2026, 15(8): 3830-3849

ISSN: 2277–4998

International Journal of Biology, Pharmacy and Allied Sciences (IJBPAS)

'A Bridge Between Laboratory and Reader'

www.ijbpas.com

INVESTIGATING THE ROLE OF BIOACTIVE COMPOUNDS FROM SWEET WORMWOOD IN RESTORING FUNCTIONALITY OF P53 IN CASES OF ORAL SQUAMOUS CELL CARCINOMA TRIGGERED BY R280K MUTATION

ROY S[1*], MUKHERJEE S[2], BANERJEE A[3] AND CHOUDHURY L[4]

[1]Assistant Professor, Post-Graduate & Research Department of Biotechnology, St. Xavier's College (Autonomous), 30, Mother Teresa Sarani, Kolkata-700 016, West Bengal, India; **ORCID ID: 0000-0001-5102-1889**

[2, 3]5th Year Integrated M.Sc. (5 Year Integrated) student, Post-Graduate & Research Department of Biotechnology, St. Xavier's College (Autonomous), 30, Mother Teresa Sarani, Kolkata-700016, West Bengal, India; **ORCID ID: 0000-0002-4011-1851; ORCID ID: 0009-0009-2416-7896**

[4]State-Aided College Teacher, Department of Microbiology, Sarsuna College (under Calcutta University), 4/HB/A, Ho-Chi-Minh Sarani, Sarsuna Upanagari, Kolkata – 700061, West Bengal, India; **ORCID ID: 0000-0002-0519-8904**

***Corresponding Author: Dr. Souvik Roy: E Mail: souvikroybiotech@sxccal.edu**

Received 25th July 2025; Revised 20th Sept. 2025; Accepted 5th Jan. 2026; Available online 1st Aug. 2026

https://doi.org/10.31032/IJBPAS/2026/15.8.10395

ABSTRACT

Abstract: Sweet wormwood (scientifically termed as *Artemisia annua)* contains bioactive compounds with diverse pharmacological activities, including anticancer properties. This study explores interactions between specific bioactive compounds from *A. annua* and the tumour suppressor protein p53 in oral squamous cell carcinoma (OSCC). The p53 protein, crucial for preventing cancer, regulates cell cycle arrest, DNA repair, apoptosis, and senescence, associating with the DNA through its DNA-binding domain (DBD). The research focuses on OSCC caused by R280K mutation in p53, evaluating the potential of these compounds to induce apoptosis by restoring original function of wild type p53. Toxicity and drug-likeness were assessed using Lipinski's Rule of Five. Structural analysis of p53, prediction of its active sites, was performed via the COACH server, followed by molecular docking to predict the binding affinity between mutant p53 DBD and the bioactive compounds. The results identified Luteolin as the most promising compound, showing significant interactions with p53 DBD, while Flaviolin demonstrated lower affinity. A 100 ns Molecular Dynamics (MD) simulation

was conducted with the best docked conformation of Luteolin. This study provides insights into the potential of *A. annua* compounds in modulating apoptosis pathways, laying the groundwork for further *in vivo* experiments in OSCC.

Keywords: *Artemisia annua*, bioactive compounds, molecular docking, molecular dynamics simulation, p53

1. INTRODUCTION

Accounting for over 90% of all cases of oral cancer detected worldwide **[1]**, oral squamous cell carcinoma (OSCC) has firmed its position as the most prevalent oral malignancy diagnosed in India, and ranks as the sixth most common cancer globally **[2]**. While chemotherapy remains a cornerstone in various cancer treatments, including OSCC, the emergence of chemotherapeutic resistance often leads to therapeutic failure and potential mortality **[3]**. Recent studies have highlighted the potential of natural bioactive compounds rich in flavonoids and polyphenols to mitigate the risk of OSCC, owing to an abundance of phytochemicals with prominent anticancer properties **[4]**. Hence, medicinal plants harboring such properties present promising avenues for OSCC treatment and management.

In Indian folklore, *Artemisia annua* is often referred to as "The Sweet Annie" **[5]**. There is a growing recognition of this plant in India as a source of herbal medicine, thanks to its huge repertoire of bioactive compounds renowned for their anticancer properties **[6]**. Previous research has demonstrated the ability of bioactive compounds from *A. annua* to chemically interact with OSCC cell lines, thereby inhibiting cell proliferation akin to certain anticancer drugs **[7]**. Consequently, these bioactive compounds hold potential in inducing programmed cell death (PCD) by activating p53 tumour suppressor proteins and other proteins associated with the apoptosis pathway **[8]**.

OSCC involves the intricate interplay of tumour suppressor genes, proto-oncogenes, and oncogenes, with mutations in the p53 gene being a common occurrence, as observed in various human cancers **[9]**. Despite ongoing evaluation, the precise role of p53 in tumorigenesis and its prognostic implications remain ambiguous **[10]**. This complexity poses challenges in identifying molecular targets for effective chemotherapeutic intervention. Molecular docking studies have emerged as a valuable tool to expedite anticancer research, particularly targeting p53, known as the tumour suppressor protein **[11]**. The multifaceted functions of p53 include halting cancer progression by cell cycle arrest through p21, regulating DNA repair

mechanisms, and inducing apoptosis via extrinsic and intrinsic pathways **[12]**.

In most cases of cancer (ranging from 65% to 85%), mutations in the p53 protein are prevalent, resulting in loss of tumour suppressor function and gain of proto-oncogenic properties, thereby promoting cancer cell progression and tumorigenesis **[9, 13]**. One such mutation is the R280K mutation **[14]**. Notably, mutated p53 can exert dominant-negative activity by oligomerization, thereby inactivating wild-type p53 function **(Figure 1) [15]**. Cancer cases with overexpressed mutated p53 often display resistance to conventional chemotherapy drugs, such as cisplatin, doxorubicin, and temozolomide **[16]**. Furthermore, specific hotspot codons within the p53 protein confer resistance to cisplatin-based chemotherapy, leading to unfavourable clinical outcomes **[11]**. Therefore, understanding the mutational status of p53 is crucial for prognosis and tailoring appropriate OSCC treatments.

Molecular docking and molecular dynamics (MD) simulation studies offer insights into protein-ligand interactions, ligand-binding mechanisms, and the stability of protein-ligand complexes **[17]**. Targeting the apoptosis pathway via *in silico* analyses presents a promising strategy to overcome drug resistance in OSCC chemotherapy. OSCC cells with p53 alterations proceed into the synthesis (S)-phase and produce damaged DNA **[1]**. Consequently, these cells fail to initiate the apoptosis pathway, leading to the gradual accumulation of cells with damaged DNA, and the formation of OSCC cell clones that progress into more aggressive carcinomas **[8]**. Hence, targeting p53 with bioactive compounds holds potential of inhibiting the mutant p53. The inhibition of mutant p53 protein can eliminate its dominant-negative effects on wild-type p53 and restore the balance of p53-mediated tumour suppression pathways, triggering apoptosis and combating OSCC progression.

This novel study elucidates the interaction between bioactive compounds derived from *A. annua* and the tumour suppressor protein p53 within the apoptosis pathway. The selected bioactive compounds were made to undergo rigorous validation for toxicity, drug-likeness, and adherence to Lipinski's Rule of Five. Subsequently, molecular docking studies were conducted to evaluate their binding affinity towards p53 protein in the apoptosis pathway. The MD simulation even unveiled the temporal evolution of the interaction, shedding light on dynamic structural changes, and the stability of the complex over the simulation period.

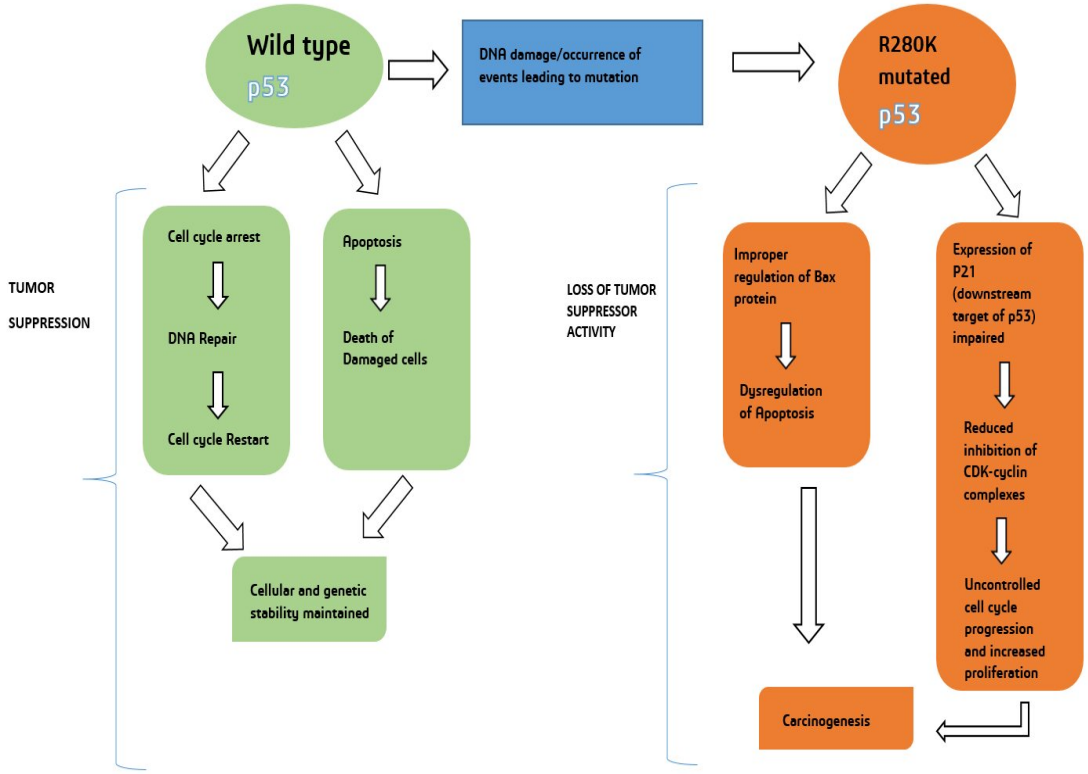

Figure 1: Functioning of wild type-p53 and R280K mutant p53

2. METHODS

2.1 Protein Model, Tertiary Structure, and Prediction of Active Site

The R280K mutant structure of p53 (PDB ID: 6FF9) having Zn(II) ions and 336 water molecules (taken into consideration) was obtained from the Research Collaboratory for Structural Bioinformatics–Protein Data Bank (RCSB-PDB) **[18]**. The protein data was saved in .pdb file format and subjected to side chain removal, elimination of water, hetatm, and ligand molecules using BIOVIA Discovery Studio 2021 Client **[19]**. PyMOL 3.0 was utilized to predict the tertiary structure of the protein **[20]**. The identification of active sites within the protein structure was performed using the COACH server, enhancing the evaluation of the protein **[21]**.

2.2 Selection of Compounds

From a larger library of 578 compounds, based on a comprehensive literature review, seven bioactive compounds from *Artemisia annua* were chosen **[6, 22, 23]**. The 3D structures of these compounds were retrieved from the PubChem database in SDF file format and subsequently converted to .pdbqt file format using the Open babel plugin of PyRx software **[24]**.

2.3 Toxicity and Drug Likeness Prediction

The drug-likeness of compounds was evaluated utilizing Lipinski's Rule of Five **[25, 26]**. This rule predicts compound

infusion or incorporation based on parameters such as calculated logP (ClogP) > 5.37, molecular weight (MW) > 500 g/mol, and presence of more than 10 acceptors and five donors of hydrogen bonds **[27]**. Compound selection was further guided by their drug score values, with higher scores indicating superior drug candidacy **[28]**. Screening of bioactive compounds was conducted using the Swiss ADME predictor, providing insights into parameters such as the number of rotatable bonds, hydrogen acceptors, and hydrogen donors, ensuring adherence to Lipinski's Rule of Five for subsequent molecular docking studies **[29]**.

2.4 Molecular Docking

Molecular docking analysis was performed using PyRx **[24]**. Polar hydrogen atoms and Gasteiger partial charges were incorporated into the protein structure, which was then saved in .pdbqt file format for analysis. Active sites/DNA binding domain (DBD) within the protein, as predicted by the COACH server, were selected to set the grid box accordingly. Lamarckian Genetic Algorithm 4.2 was employed for docking studies, with the protein macromolecule maintained rigid throughout the process. Genetic algorithm runs were set at 30, with default parameters for docking analysis. The best protein-ligand conformations were determined based on Auto Dock 1.5.6 scoring function (PyRx uses the Autodock vina engine), with rankings assigned according to their binding affinities. The best conformations for each ligand having Root Mean Square Deviation (upper bound) and Root Mean Square Deviation (lower bound) (RMSD/ub and RMSD/lb values respectively) were considered. Post-docking analysis was conducted using BIOVIA Discovery Studio 2021 Client and PyMOL 3.0 **[21]**.

2.5 Performance of Structural Alignment

Structural alignment was conducted using PyMOL between the wild-type functional p53 (PDB: 1TUP) and the R280K mutant p53 (PDB: 6FF9). Following the docking of Luteolin into the DNA-binding domain (DBD) of the R280K mutant p53, a subsequent structural alignment was performed. This alignment compared the best-docked conformation of the Luteolin-R280K p53 complex with the wild-type functional p53 to evaluate the restoration of the native functional conformation of p53, enabling DNA binding and tumour suppressor activity.

2.6 Molecular Dynamics (MD) Simulation

The best docked bioactive compound underwent molecular dynamics (MD) simulation using the GROMACS software **[30]**. GROMACS, a versatile molecular dynamics simulation package, was employed to explore the dynamic behaviour of the docked complex over a

100-nanoseconds (ns) period. Parameters for the MD simulation were set to reflect physiological conditions, utilizing the CHARMM36 force field **[31]**. The system was solvated in a cubic water box, and counter-ions were added to neutralize the charge **[30]**. The simulation allowed for the examination of structural stability, flexibility, and dynamic interactions of the best docked bioactive compound **[18]** providing valuable insights into potential therapeutic strategies for p53-associated cancers and guiding the development of anti-cancer drugs.

3. RESULTS

3.1 Tertiary structure analysis

The p53 gene is located on chromosome 17p13.1 of humans, encoding a 53-kDa, 393 amino acid (AA) sequence region with nuclear phosphoproteins known for cell proliferation and regulation of cell growth **[32]**. The human p53 protein consists of four major functional domains within its 393 amino acids. At the C-terminal portion, there is an oligomerization domain (AAs 323–356) and a regulatory domain (AAs 360–393). At the N-terminus lies a transcriptional activation domain (AAs 1–42), and within the central part of p53 resides the sequence-specific DNA-binding domain (AAs 102–292). It is important to note that specific mutations, such as the R280K mutation, can occur within this DNA-binding domain, impacting its functionality **[33]**.

3.2 Prediction of drug-likeness

Swiss ADME web server predicts the physiochemical factors of the ligands as shown in **Table 1**. Lipinski's Rule of Five was used for filtration and screening of ligands, and seven potential active bioactive compounds with anti-cancer properties were left as it is. Generally, Lipinski's Rule states that an orally active drug cannot violate more than one of Lipinski's Rule parameters. One among the seven bioactive compounds does not satisfy Lipinski's Rule, which is l-(+)-Ascorbic acid 2,6-dihexadecanoate with two violations as MW is > 500 g/mol, i.e., 652.94 g/mol and iLogP> 5, i.e. 7.58. All other bioactive compounds satisfied Lipinski's Rule of Five. After screening with Lipinski's Rule of Five, six compounds were taken for further docking study **(Table 2)**.

Table 1: Lipinski's Rule for *A. annua*-Derived Bioactive Compounds by Swiss Adme Server; Bold Represents Violations From the Rule

Ligands	iLogP < 5	Molecular Weight (g/mol) < 500	Hydrogen Acceptor < 10	Hydrogen Donor < 5	Drug-likeness Lipinski's rule follows	Violation
Quercetin	**1.63**	**302.24**	**7**	**5**	**Yes**	**0**
Luteolin	**1.86**	**286.24**	**6**	**4**	**Yes**	**0**
Flaviolin	**0.36**	**206.15**	**5**	**3**	**Yes**	**0**
Rhamnetin	**2.23**	**316.26**	**7**	**4**	**Yes**	**0**
Pilloin	**4.33**	**314.29**	**6**	**2**	**Yes**	**0**
Kaempferol	**1.70**	**286.24**	**6**	**4**	**Yes**	**0**
l-(+)-Ascorbic acid 2,6-dihexadecanoate	**7.58**	**652.94**	**8**	**2**	**No**	**2**

3.3 Active-site and DBD prediction

The active site/DBD prediction of targeted p53 protein was done with COACH server. The grid box was centred at the predicted DBD (of the R280K mutant p53) for further docking study to identify inhibitory potential of these bioactive compounds.

3.4 Molecular docking

The targeted p53 protein is docked with six potential bioactive compounds which are validated by Swiss ADME. **Table 2** indicates the binding affinity for each compound with targeted apoptosis protein. The docking pattern of each bioactive compound after docking with p53 was analyzed using AutoDock 1.5.6, and the docking of the bioactive compounds with active site residues of protein was analyzed using PyMol 3.0 and Discovery studio Visualizer 4.1 client. The bioactive compounds showed varying degrees of favorable docking with the targeted protein p53. As l-(+)-Ascorbic acid 2,6-dihexadecanoate had two violations, and did not satisfy Lipinski's Rule, no further docking study was done with this compound. After docking, it was found that Luteolin had a high binding affinity towards p53 (–7.40 kcal/mol), whereas the lowest binding affinity detected was –5.80 for Flaviolin **(Table 2)**.

Protein-ligand docking analysis showed that Luteolin had an adequate binding affinity towards p53. There are 4 H-bonding observed between p53 and Luteolin; two bonds with PHE-113 and HIS-115 respectively, and one bond with SER-269. Quercetin, Rhamnetin, Pilloin and Kaempferol formed six, six, four and two H-bonds respectively. Flavilin showed the lowest binging affinity towards p53, hence formed only one H- bond with ASN-200 **(Table 2, Figure 2)**.

Table 2: Results of Molecular Docking of p53 With The Bioactive Compounds (Which Obey Lipinski's Rule of 5)

Targeted Protein	Bioactive Compound	Structure	No. of H-bonds	Interacting Residues	Distance (Å)	Binding Affinity (kcal/mol)
p53	Quercetin (PubChem CID 5280343)	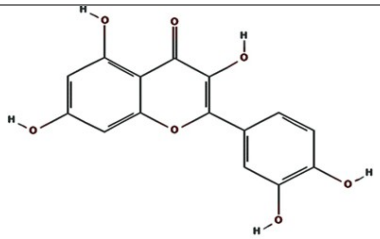	6	SER-269, PHE-113, HIS-115	2.0, 2.3, 2.3, 2.4, 2.6, 2.9	-7.10
	Luteolin (PubChem CID 5280445)	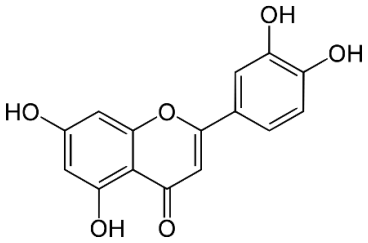	4	SER-269, PHE-113, HIS-115	2.1, 2.1, 2.2, 2.6	-7.40
	Flaviolin (PubChem CID 160478)	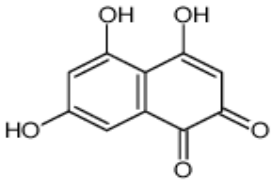	1	ILE-232, GLU-221, ASN-200	2.3	-5.80
	Rhamnetin (PubChem CID 5281691)	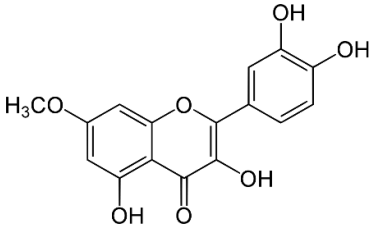	6	THR-231, PRO-222, ILE-232, VAL-218	1.9, 2.3, 2.6, 2.6, 3.2, 3.7	-6.70
	Pilloin (PubChem CID 5320496)	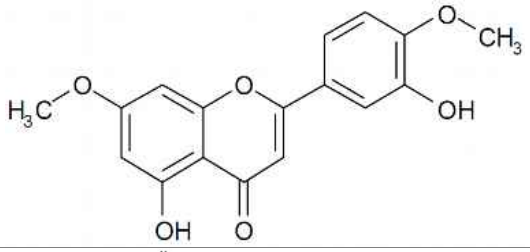	4	PHE-113, HIS-115	2.2, 2.4, , 2.5, 3.1	-6.70
	Kaempferol (PubChem CID 5280863)	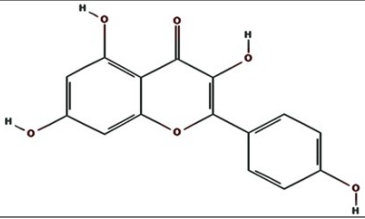	2	SER-269, HIS-115	2.3, 2.4	-6.60

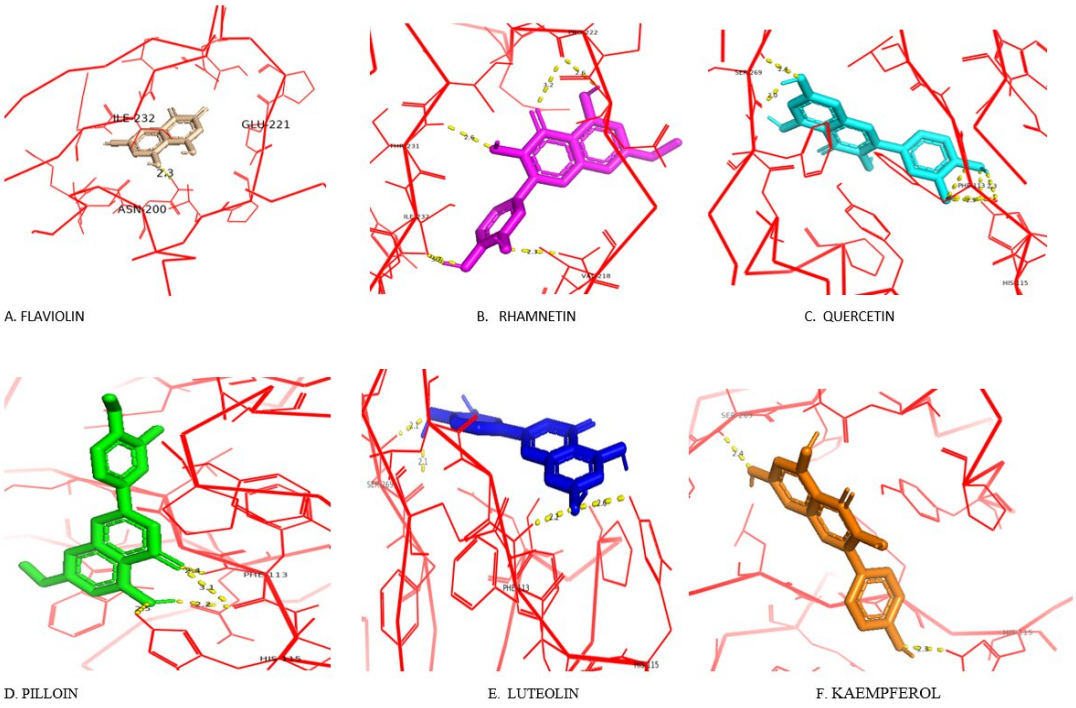

Figure 2: p53 DBD interacting with the *Artemisia annua* derived bioactive compounds (best docked conformation)

3.5 Structural Alignment of docked complex with functional p53

Structural alignment in PyMOL between the wild-type functional p53 and the R280K mutant p53 revealed a root mean square deviation (RMSD) of **3.2 Å**, highlighting significant structural alterations in the mutant. Key deviations were observed in the DNA-binding domain, particularly in the orientation of critical residues such as Arg248 and Lys120, which are essential for stable DNA interaction. The R280K mutation disrupts hydrogen bonding and electrostatic interactions required for maintaining the native conformation, thereby compromising the protein's ability to bind DNA and execute its tumour suppressor functions.

Further structural alignment between the wild-type p53 and the best-docked conformation of the Luteolin-R280K p53 complex showed an RMSD of **0.8 Å**, indicating a high degree of structural resemblance to the wild-type functional p53. Remarkably, Luteolin docking appeared to restore the positioning of key residues, re-establishing the hydrogen bonds and electrostatic interactions necessary for DNA binding. This finding demonstrates that Luteolin docking effectively restores the native functional conformation of the p53 protein, enabling it to bind DNA and fulfill its tumour suppressor role.

3.6 Molecular Dynamics (MD) Simulation Results

The 100-ns MD simulation of the Luteolin-p53 DBD complex delved into its dynamic structural behaviour **(Figure 3)**. Commencing with an initial total energy of -264426 kJ/mol, the simulation captures fluctuations in stability, revealing dynamic flexibility and structural changes. The RMSD (Root mean square deviation), RMSF (Root mean square fluctuation) and Rg (Radius of gyration) of Luteolin relative to p53 DBD, and total energy graphs for the complex, collectively presented a concise overview of the intricate molecular dynamics, setting the stage for an in-depth analysis of potential therapeutic strategies targeting p53-associated cancers.

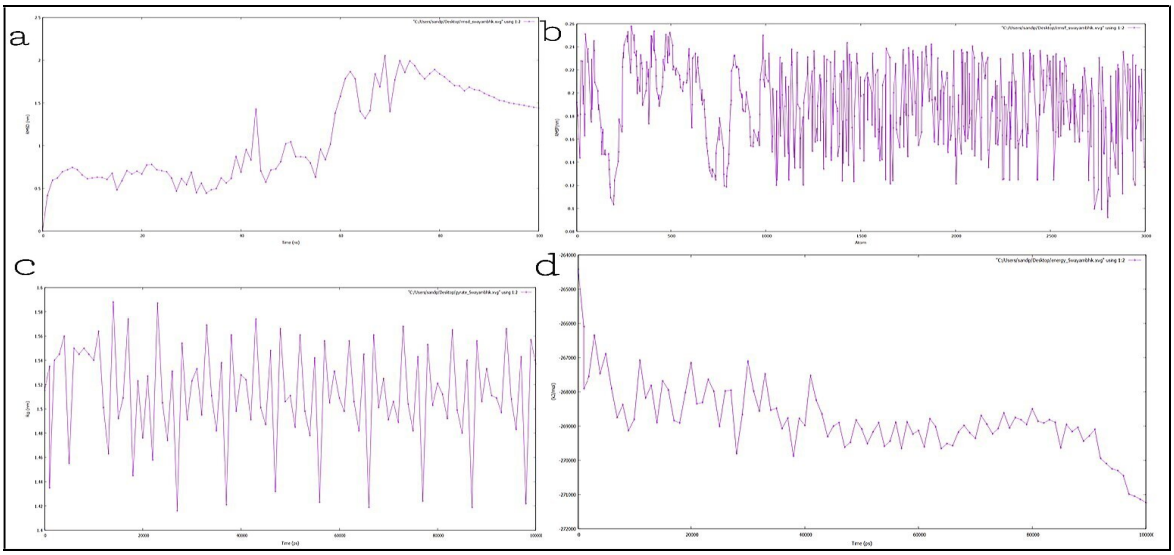

Figure 3: MD simulation-generated graphs of: a RMSD; b RMSF; c Rg; d Total energy

The comprehensive RMSD analysis **(Figure 3a)** of the MD simulation spanning 100 ns or 100000 picoseconds (ps) provides crucial insights into the stability and dynamics of the Luteolin and p53 DBD complex. The analysis is suggestive of three phases. In the phase of initial stability (0-60 ns), the RMSD values consistently maintained levels below 1.5 Å, reflecting a robust and stable interaction between Luteolin and the p53 DBD. Minor fluctuations observed during this phase suggest subtle conformational adjustments, ensuring a steadfast interaction throughout. In the phase of transitory structural rearrangement (60-80 ns), beyond the initial 60 ns, a slight increase in RMSD was noted, indicating minor structural rearrangements within the complex. The RMSD values rose slightly above 2 Å, suggesting transient deviations from the initial conformation. In the phase of recovery and sustained stability (80-100 ns), subsequent to the transient increase, the RMSD values demonstrated a decline, signifying a return to more stable interactions. Throughout the simulation, RMSD values consistently remained below

2.5 Å, indicating highly stable and favourable interactions between best docked conformation of Luteolin and p53 DBD. The observed RMSD patterns aligned well with literature, where RMSD values below 3.0 Å were considered indicative of stable protein-ligand interactions **[34]**. The results strongly supported the conclusion that the Luteolin and p53 DBD complex maintains a highly steady conformation, particularly during the crucial initial 60 ns. The analysis also highlighted the resilience of the complex, even during transient structural rearrangements, emphasizing its potential as a stable platform for targeted therapeutic interventions.

The RMSF graph **(Figure 3a)** presented a noteworthy depiction of the dynamic behaviour and flexibility of distinct regions within the Luteolin-p53 DBD complex. Throughout the 100 ns simulation, the RMSF values always remained below the threshold **[35]** of 0.30 nm (3.0 Å) for all atoms, indicating a remarkable level of stability and limited fluctuations in atomic positions within the complex. Examining the initial 1000 of the atoms, a cyclic pattern of increase and decrease in RMSF values was discernible, representing a certain amount of flexibility among different regions within this subset of the complex. While fluctuations were observed, the pace is relatively moderate, underscoring a measured and controlled level of flexibility. Moving to the subset of 1000 to 2995 of the atoms, cyclic pattern became more rapid, suggesting intensified local structural adjustments within this subset. Despite the increased speed of fluctuations, the RMSF values (very notably) for these atoms consistently remained below 0.26 nm (2.6 Å), highlighting a high degree of stability and favourable interactions. This heightened stability observed in both subsets of atoms accentuated the controlled nature of interactions within the Luteolin-p53 DBD complex.

The Rg was employed as a metric to assess the compactness and overall structural stability. The Rg values **(Figure 3c)**, ranging from 1.41 nm to 1.59 nm, depicted a dynamic profile of the complex's overall size throughout the simulation. Notably, the majority of Rg values fell within a tight range of 1.46 nm to 1.56 nm, indicating a consistent and well-defined structural state. If the Rg graph was drawn to less detailed y-axis scale (having a higher value difference between two consecutive points in the y-axis), most of the graph would represent a plateau **(Figure 4)**. The occurrence of this kind of typical plateau in Rg graph aligned with the literature definitions of stable Rg in an MD simulation **[36]**. This limited variability suggested that the complex maintained a

relatively constant compactness, once again underscoring the stability of the Luteolin and p53 DBD interaction. The absence of Rg values exceeding 1.6 nm throughout the simulation duration further underscored the stability of the Luteolin and p53 DBD complex. This result was consistent with literature expectations, where an Rg value below 1.6 nm is indicative of a structurally stable macromolecular complex **[37]**.

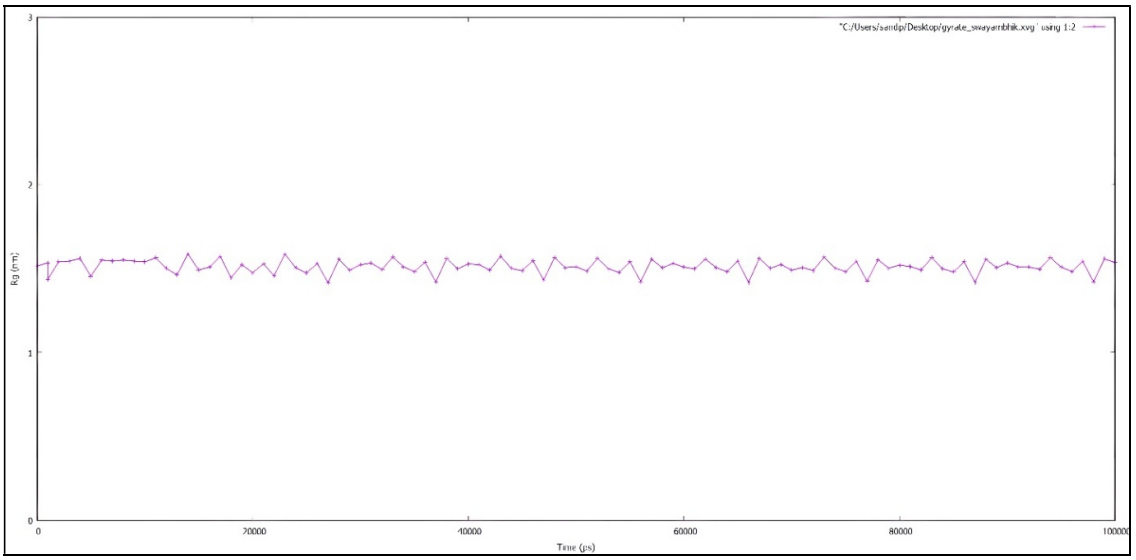

Figure 4: The same Rg graph as Figure 3c in a less detailed y-axis scale of 1 nm difference in contrast to the previous 0.02 nm difference between two successive data points on y-axis. This graph typically represents the 'plateau' form

The total energy of the complex was monitored throughout the 100000 ps (100 ns) simulation to gain insights into the energetics and stability of the system. At the initiation of the simulation, the total energy was recorded as -264426 kJ/mol **(Figure 3d)**, serving as the baseline energy state for the complex. Throughout the simulation, a consistent pattern of energy decrease was observed. Despite minor fluctuations, the overall trajectory displayed a clear trend of diminishing total energy, reaching -271237 kJ/mol by the conclusion of the 100 ns **(Figure 3d)**. The negative sign in the total energy values indicated the energetic favourability of the ligand-protein complex, and the sustained decrease underscored a persistent drive towards a more stable configuration. The minor ups and downs in the energy graph may correspond to transient fluctuations and adjustments within the complex, but the overarching trend of decreasing total energy implied a systematic process of energy minimization. This phenomenon suggested that the ligand-protein complex actively sought a more energetically favourable conformation or state over the simulation duration. The final total energy value of -271237 kJ/mol signified that the complex achieved a lower energy state, indicating a more stabilized and

energetically-favoured configuration at the termination of the 100 ns MD simulation. This observation aligned with the expectations of a system undergoing energy minimization and structural stabilization.

4. DISCUSSIONS

According to Lipinski's Rule of Five, a compound should have a molecular weight of less than 500 g/mol, a lipophilicity (iLogP) of less than 5, fewer than 5 hydrogen bond donors, and fewer than 10 hydrogen bond acceptors. These parameters are closely related to intestinal permeability and solubility, which are crucial factors in oral bioavailability. Additionally, if a compound violates these parameters twice or more times, it is unlikely to be a viable drug molecule **[26]**. Bioactive compounds selected for docking analysis adhered to Lipinski's Rule of Five, with iLogP values less than five and specific hydrogen bond donor counts. However, some compounds, such as l-(+)-Ascorbic acid 2,6-dihexadecanoate, violated Lipinski's Rule by having molecular weights exceeding 500 g/mol and excessive iLogP value. Flaviolin exhibited only one hydrogen bonding with the p53 protein, indicating minimal interaction. Toxicity considerations, which can override ADME parameters, are crucial in drug development, as adverse effects from toxicity can lead to drug failure during clinical trials **[38]**. Molecular docking results provide insights into the binding affinity between proteins and ligands, with lower binding energy indicating stronger interactions. In this study, luteolin demonstrated the highest binding affinity of -7.40 kcal/mol with p53 DBD.

Previous researches suggested that bioactive compounds from *A. annua* inhibit malignant cell proliferation, induce cancer cell death, and increase p53 protein levels. Quercetin and Rhamnetin formed multiple hydrogen bonds during docking, while Quercetin and Luteolin exhibited similar bonding patterns, albeit with very minimum variations in bond distances.

The RMSD value of 0.8 Å (indicative of highly similar structures) obtained from the structural alignment of Luteolin-R280K p53 and wild type p53 indicates a restoration of the functional conformation of p53.

Furthermore, the MD simulation in this study offered a dynamic perspective on the structural behaviour of the Luteolin-p53 DBD complex over a 100-ns period. The simulation revealed stable interactions between Luteolin and p53, with minor fluctuations in structural stability observed throughout the simulation. The RMSD analysis indicated that the complex maintained a highly stable conformation, particularly during the initial 60 ns, highlighting the robustness of the Luteolin-p53 interaction. The RMSF analysis

provided insights into the dynamic flexibility of distinct regions within the Luteolin-p53 DBD complex, demonstrating a remarkable level of stability and limited fluctuations in atomic positions. The Rg analysis further underscored the stability of the complex, with Rg values consistently falling within a tight range, indicative of a well-defined structural state. Additionally, the total energy analysis revealed a systematic decrease in energy over the simulation duration, indicating a persistent drive towards a more stable configuration of the complex.

In summary, Luteolin emerged as the most favourable candidate against p53, indicating its potential efficacy in cancer treatment. However, different analysis tools or software may yield differing outcomes due to algorithmic variations **[39]**. Additionally, discrepancies in protein data across databases highlight the importance of methodological consistency **[40]**.

Future research directions in this regard may include comparing protein structures from various databases, evaluating *in vitro* and *in vivo* protein and gene expression, and validating *in silico* findings. OSCC arises from damaged areas that lose their repair capability, often due to mutated p53 protein. Herbal medications like *A. annua*-derived compounds, particularly Luteolin, offer promising avenues for OSCC treatment by targeting p53, and inducing apoptosis in cells with damaged DNA.

5. CONCLUSION

This novel study elucidates the potential of Luteolin, a bioactive compound from *Artemisia annua*, in targeting p53, for the treatment of oral squamous cell carcinoma (OSCC). Luteolin demonstrated the strongest binding affinity among all other bioactive compounds, helped in restoration of the native functional conformation of p53 upon binding to mutant DBD and showed a notable structural stability with p53 over a 100 ns simulation period, suggesting its efficacy in inducing apoptosis in OSCC cells. Luteolin adhered to all the parameters laid down by Lipinski's rule of five, enhancing its candidacy as a drug molecule. Future research should focus on validating these *in silico* findings through *in vitro* and *in vivo* experiments, further solidifying Luteolin's potential as a therapeutic agent for OSCC.

6. ACKNOWLEDGEMENT

The authors express their deepest gratitude to Rev. Dr. Dominic Savio, SJ, Principal, St. Xavier's College, Kolkata (Autonomous) and Smt. Prashasti Bhattacharyya, Vice Principal, Sarsuna College, Kolkata.

7. CONFLICT OF INTEREST

The authors declare no potential conflict of interest.

8. REFERENCES

[1] Badwelan, M.; Muaddi, H.; Ahmed, A.; Lee, K.T.; Tran, S.D. (2023). Oral Squamous Cell Carcinoma and Concomitant Primary Tumors, What Do We Know? A Review of the Literature. Current Oncology, 30, 3721-3734. https://doi.org/10.3390/curroncol30040283

[2] Borse V, Konwar AN, Buragohain P. (2020). Oral cancer diagnosis and perspectives in India. Sensors International, 1, 100046. https://doi.org/10.1016/j.sintl.2020.100046

[3] Alfarouk KO, Stock CM, Taylor S, Walsh M, Muddathir AK, Verduzco D, *et al*. (2015). Resistance to cancer chemotherapy: failure in drug response from ADME to Pgp. Cancer Cell International, 15, 71. https://doi.org/10.1186/s12935-015-0221-1

[4] Kumar, M., & Jha, A. K. (2023). Exploring the potential of dietary factors and plant extracts as chemopreventive agents in oral squamous cell carcinoma treatment. Frontiers in oral health, 4, 1246873. https://doi.org/10.3389/froh.2023.1246873

[5] Septembre-Malaterre, A., Lalarizo Rakoto, M., Marodon, C., Bedoui, Y., Nakab, J., Simon, E., Hoarau, L., Savriama, S., Strasberg, D., Guiraud, P., Selambarom, J., & Gasque, P. (2020). *Artemisia annua*, a Traditional Plant Brought to Light. International journal of molecular sciences, 21(14), 4986. https://doi.org/10.3390/ijms21144986

[6] Ferreira, J.F.S.; Luthria, D.L.; Sasaki, T.; Heyerick, A. (2010). Flavonoids from *Artemisia annua* L. as Antioxidants and Their Potential Synergism with Artemisinin against Malaria and Cancer. Molecules, 15, 3135-3170. https://doi.org/10.3390/molecules15053135

[7] Khan, T., Ali, M., Khan, A., Nisar, P., Jan, S. A., Afridi, S., & Shinwari, Z. K. (2019). Anticancer Plants: A Review of the Active Phytochemicals, Applications in Animal Models, and Regulatory Aspects. Biomolecules, 10(1), 47. https://doi.org/10.3390/biom10010047

[8] He, S., Chakraborty, R., & Ranganathan, S. (2022). Proliferation and Apoptosis Pathways and Factors in Oral Squamous Cell Carcinoma.

International journal of molecular sciences, 23(3), 1562. https://doi.org/10.3390/ijms23031562

[9] Choudhary, H. B., Mandlik, S. K., & Mandlik, D. S. (2023). Role of p53 suppression in the pathogenesis of hepatocellular carcinoma. World journal of gastrointestinal pathophysiology, 14(3), 46–70. https://doi.org/10.4291/wjgp.v14.i3.46

[10] Wallis, B., Bowman, K. R., Lu, P., & Lim, C. S. (2023). The Challenges and Prospects of p53-Based Therapies in Ovarian Cancer. Biomolecules, 13(1), 159. https://doi.org/10.3390/biom13010159

[11] Wang, H., Guo, M., Wei, H. *et al*. (2023). Targeting p53 pathways: mechanisms, structures, and advances in therapy. Signal Transduction and Targeted Therapy, 8, 92. https://doi.org/10.1038/s41392-023-01347-1

[12] Abuetabh, Y., Wu, H. H., Chai, C., Al Yousef, H., Persad, S., Sergi, C. M., & Leng, R. (2022). DNA damage response revisited: the p53 family and its regulators provide endless cancer therapy opportunities. Experimental & molecular medicine, 54(10), 1658–1669. https://doi.org/10.1038/s12276-022-00863-4

[13] Lindemann A, Takahashi H, Patel AA, Osman AA, Myers JN. (2018). Targeting the DNA Damage response in OSCC with TP53 mutations. Journal of Dental Research, 97, 635-644. https://doi.org/10.1177/0022034518759068

[14] Counihan, J. L., Grossman, E. A., & Nomura, D. K. (2018). Cancer Metabolism: Current Understanding and Therapies. Chemical Reviews, 118(14), 6893–6923. https://doi.org/10.1021/acs.chemrev.7b00775

[15] Michael J. Duffy, Naoise C. Synnott, Shane O'Grady, John Crown. (2022). Targeting p53 for the treatment of cancer, Seminars in Cancer Biology, 79, 58-67. https://doi.org/10.1016/j.semcancer.2020.07.005

[16] Hassin, O., Oren, M. (2023). Drugging p53 in cancer: one protein, many targets. Nature Reviews Drug Discovery, 22, 127–144. https://doi.org/10.1038/s41573-022-00571-8

[17] Challapa-Mamani, M.R.; Tomás-Alvarado, E.; Espinoza-Baigorria, A.; León-Figueroa, D.A.; Sah, R.; Rodriguez-Morales, A.J.; Barboza, J.J. (2023). Molecular Docking and Molecular Dynamics Simulations in Related to *Leishmania donovani*: An Update and Literature Review. Tropical Medicine and Infectious Disease, 8, 457. https://doi.org/10.3390/tropicalmed8100457

[18] Gomes, A. S., Trovão, F., Andrade Pinheiro, B., Freire, F., Gomes, S., Oliveira, C., Domingues, L., Romão, M. J., Saraiva, L., & Carvalho, A. L. (2018). The crystal structure of the R280K mutant of human p53 explains the loss of DNA binding. International Journal of Molecular Sciences, 19(4), 1184. https://doi.org/10.3390/ijms19041184

[19] Haque, A., Baig, G. A., Alshawli, A. S., Sait, K. H. W., Hafeez, B. Bin, Tripathi, M. K., Alghamdi, B. S., Mohammed Ali, H. S. H., & Rasool, M. (2022). Interaction Analysis of MRP1 with Anticancer Drugs Used in Ovarian Cancer: In Silico Approach. Life, 12(3), 383. https://doi.org/10.3390/life12030383

[20] Janson, G., & Paiardini, A. (2021). PyMod 3: A complete suite for structural bioinformatics in PyMOL. Bioinformatics, 37(10), 1471–1472. https://doi.org/10.1093/bioinformatics/btaa849

[21] Wu, Q., Peng, Z., Zhang, Y., & Yang, J. (2018). COACH-D: improved protein-ligand binding sites prediction with refined ligand-binding poses through molecular docking. Nucleic acids research, 46(W1), W438–W442. https://doi.org/10.1093/nar/gky439

[22] Singh, P., Bajpai, V., Khandelwal, N., Varshney, S., Gaikwad, A. N., Srivastava, M., Singh, B., & Kumar, B. (2021). Determination of bioactive compounds of *Artemisia* sSpp. plant extracts by LC-MS/MS technique and their in-vitro anti-adipogenic activity screening. Journal of pharmaceutical and biomedical analysis, 193, 113707. https://doi.org/10.1016/j.jpba.2020.113707

[23] Anibogwu, R., Jesus, K., Pradhan, S., Pashikanti, S., Mateen, S., & Sharma, K. (2021). Extraction, Isolation and Characterization of

Bioactive Compounds from Artemisia and Their Biological Significance: A Review. Molecules (Basel, Switzerland), 26(22), 6995. https://doi.org/10.3390/molecules26226995

[24] Oyedele, A. K., Adelusi, T. I., Ogunlana, A. T., Adeyemi, R. O., Atanda, O. E., Babalola, M. O., Ashiru, M. A., Ayoola, I. J., & Boyenle, I. D. (2022). Integrated virtual screening and molecular dynamics simulation revealed promising drug candidates of p53-MDM2 interaction. Journal of molecular modeling, 28(6), 142. https://doi.org/10.1007/s00894-022-05131-w

[25] Lipinski CA, Lombardo F, Dominy BW, Feeney PJ. (2001). Experimental and computational approaches to estimate solubility and permeability in drug discovery and development settings. Advanced Drug Delivery Reviews, 46, 3-26. https://doi.org/10.1016/s0169-409x(00)00129-0

[26] Lipinski CA. (2004). Lead- and drug-like compounds: the rule-of-five revolution. Drug Discovery Today: Technologies, 1, 337-341. https://doi.org/10.1016/j.ddtec.2004.11.007

[27] de Brito MA. (2011). Pharmacokinetic study with computational tools in the medicinal chemistry course. Brazilian Journal of Pharmaceutical Sciences, 47, 797-805. https://doi.org/10.1590/S1984-82502011000400017

[28] Oduselu GO, Ajani OO, Ajamma YU, Brors B, Adebiyi E. (2019). Homology modelling and molecular docking studies of selected substituted benzo[d]imidazol-1-yl)methyl)benzimidamide scaffolds on *Plasmodium falciparum* adenylosuccinate lyase receptor. Bioinformatics and Biology Insights, 13, 1177932219865533. https://doi.org/10.1177/1177932219865533

[29] Daina A, Michielin O, Zoete V. (2017). SwissADME: a free web tool to evaluate pharmacokinetics, drug-likeness and medicinal chemistry friendliness of small molecules. Scientific Reports, 7, 42717. https://doi.org/10.1038/srep42717

[30] Abraham, M. J., Murtola, T., Schulz, R., Páll, S., Smith, J. C., Hess, B., & Lindah, E. (2015). Gromacs: High performance molecular simulations through multi-level parallelism from laptops to supercomputers. SoftwareX, 1–2, 19–25. https://doi.org/10.1016/j.softx.2015.06.001

[31] Wacha, A. F., & Lemkul, J. A. (2023). charmm2gmx: An Automated Method to Port the CHARMM Additive Force Field to GROMACS. Journal of Chemical Information and Modeling, 63(14), 4246–4252. https://doi.org/10.1021/acs.jcim.3c00860

[32] Ghanghoria S, Ghanghoria A, Shukla A. (2015). p53 expression in oral cancer: a study of 50 cases. Journal of Pathology of Nepal, 5, 747-751. https://doi.org/10.3126/jpn.v5i9.13785

[33] May P, May E. (1999). Twenty years of p53 research: structural and functional aspects of the p53 protein. Oncogene, 18, 7621-7636. https://doi.org/10.1038/sj.onc.1203285

[34] Broni, E., Striegel, A., Ashley, C., Sakyi, P. O., Peracha, S., Velazquez, M., Bebla, K., Sodhi, M., Kwofie, S. K., Ademokunwa, A., Khan, S., & Miller, W. A. (2023). Molecular Docking and Dynamics Simulation Studies Predict Potential Anti-ADAR2 Inhibitors: Implications for the Treatment of Cancer, Neurological, Immunological and Infectious Diseases. International Journal of Molecular Sciences, 24(7), 6795. https://doi.org/10.3390/ijms24076795

[35] Li, M. H., Luo, Q., Xue, X. G., & Li, Z. S. (2011). Molecular dynamics studies of the 3D structure and planar ligand binding of a quadruplex dimer. Journal of Molecular Modeling, 17(3), 515–526. https://doi.org/10.1007/s00894-010-0746-0

[36] Lee, Y. H., Chatani, E., Sasahara, K., Naiki, H., & Goto, Y. (2009). A comprehensive model for packing and hydration for amyloid fibrils of β2-microglobulin. Journal of Biological Chemistry, 284(4), 2169–2175. https://doi.org/10.1074/jbc.M806939200

[37] Shrestha, A., Marahatha, R., Basnet, S., Regmi, B. P., Katuwal,

S., Dahal, S. R., Sharma, K. R., Adhikari, A., Chandra Basnyat, R., & Parajuli, N. (2022). Molecular Docking and Dynamics Simulation of Several Flavonoids Predict Cyanidin as an Effective Drug Candidate against SARS-CoV-2 Spike Protein. Advances in Pharmacological and Pharmaceutical sciences, 2022, 3742318. https://doi.org/10.1155/2022/3742318

[38] Wang, Y., Xing, J., Xu, Y., Zhou, N., Peng, J., Xiong, Z., Liu, X., Luo, X., Luo, C., Chen, K., Zheng, M., & Jiang, H. (2015). In silico ADME/T modelling for rational drug design. Quarterly reviews of biophysics, 48(4), 488–515. https://doi.org/10.1017/S0033583515000190

[39] Plewczynski, D., Łaźniewski, M., Augustyniak, R., & Ginalski, K. (2011). Can we trust docking results? Evaluation of seven commonly used programs on PDBbind database. Journal of computational chemistry, 32(4), 742–755. https://doi.org/10.1002/jcc.21643

[40] Ismail, N. Z., Mohamed, W. A. S., Ab Rahim, N., Hashim, N. M., Adebayo, I. A., Mohamad Zain, N. N., & Arsad, H. (2023). Molecular docking and molecular dynamic simulations of apoptosis proteins with potential anticancer compounds present in *Clinacanthus nutans* extract using gas chromatography-mass spectrometry. Journal of biomolecular structure & dynamics, 41(13), 6104–6120. https://doi.org/10.1080/07391102.2022.2101530